

The high-order exponential semi-implicit scalar auxiliary variable approach for nonlocal Cahn-Hilliard equation

Xiaoqing Meng^a, Aijie Cheng ^{*a}, Zhengguang Liu^b

^a*School of Mathematics, Shandong University, Jinan, Shandong 250100, China.*

^b*School of Mathematics and Statistics, Shandong Normal University, Jinan, Shandong 250014, China.*

Abstract

The nonlocal Cahn-Hilliard (NCH) equation with nonlocal diffusion operator is more suitable for the simulation of microstructure phase transition than the local Cahn-Hilliard (LCH) equation. In this paper, based on the exponential semi-implicit scalar auxiliary variable (ESI-SAV) method, the highly efficient and accurate schemes in time with unconditional energy stability for solving the NCH equation are proposed. On the one hand, we have demonstrated the unconditional energy stability for the NCH equation with its high-order semi-discrete schemes carefully and rigorously. On the other hand, in order to reduce the calculation and storage cost in numerical simulation, we use the fast solver based on FFT and FCG for spatial discretization. Some numerical simulations involving the Gaussian kernel are presented and show the stability, accuracy, efficiency and unconditional energy stability of the proposed schemes.

keywords

High-order schemes; Exponential semi-implicit scalar auxiliary variable; Nonlocal Cahn-Hilliard equation; Unconditional energy stability; Numerical simulations

1 Introduction

It is well known that LCH equation is one of the phase field models, and the history of the phase field model can be traced back to a century ago which has been applied in many fields [3, 4, 9, 12, 15, 25, 32, 36, 37]. The Cahn-Hilliard-type models are effective numerical tools for simulating interface motions between various materials [8, 10, 11, 24, 26, 27, 31, 34, 41]. The LCH is the result of the variation of the energy functional in Sobolev space H^{-1} . Furthermore, the LCH equation can be regarded as an approximation of the NCH model in which the nonlocal convolution potential is replaced by the differential term [17, 18]. For the nonlocal models, much has been done in mathematical analysis. Bates and Han [6, 7] analyzed the well-posedness of equations with Neumann and Dirichlet boundary conditions. Guan et al. pointed out in [21] that the existence and uniqueness of periodic solutions of equations can be proved by a similar technique. In order to develop a general framework for nonlocal equations, Du et al. [13] analyzed a class of nonlocal spread problems with volumetric constraint boundary conditions.

As the NCH equation gets more and more attention and is applied in many fields from physics, material science to finance and image processing [2, 11, 16, 33, 43], so it is necessary to construct some effective methods for solving the NCH equation. Due to the functional variation approach

*Corresponding author: aijie@sdu.edu.cn

used in the modeling process, the exact solution of the phase field follows the energy dissipation law, which demonstrates the thermodynamic consistency in physics and well-posedness in mathematics. Therefore, the main challenge of numerical simulation for the NCH equation is to design appropriate method to discrete nonlinear and nonlocal terms while maintaining the energy stability at the discrete level. In addition, if the numerical energy stability has no restriction with respect to the time step, it is usually called unconditional energy stability [10]. The significance of energy stability is not only important for long time accurate numerical simulation of phase field models, but also provides flexibility for dealing with stiffness problems. This property provides a lot of theoretical and practical support for efficient numerical analysis and reliable computer simulation, and is widely used in various numerical schemes of classical phase field models, such as convex splitting schemes [20, 21], stabilized schemes [39, 42], the invariant energy quadratization (IEQ) [43], the scalar auxiliary variable (SAV) methods [29], the various variants of SAV [22, 28, 30] and so on. It is also worth studying whether these various effective numerical approaches can be applied to nonlocal phase field model due to the lack of high-order diffusion term [14, 20].

Moreover, there is no doubt that, under certain precision requirements, if the expected time step is as large as possible, the high-order scheme in time is better than the lower-order scheme. This fact prompted us to develop high-order schemes, there are some existing works, such as the high-order SAV-RK (Runge-Kutta) [1, 19], SAV-GL (general linear time discretization) [40], implicit-explicit BDF k SAV [23]. All of these methods can be used to construct high-order schemes for numerical simulation of phase field models.

The purpose of this paper is to establish the high-order linear schemes (in time) for the NCH equation and prove the unconditional energy stability of the semi-discrete level, which can be naturally extended to the fully discrete setting. We adopt the exponential semi-implicit scalar auxiliary variable (ESI-SAV) approach [30], which is a novel method and has been successfully applied to solve some gradient flow and non-gradient but dissipative system. The basic idea of the ESI-SAV method is to convert the free energy into a logarithmic form of a new variable by introducing a scalar auxiliary variable (since the exponential form of the original energy is usually bounded and positive). One of the advantages of this method is that all nonlinear terms can be treated explicitly accordingly, while linear terms are treated implicitly, resulting in decoupled linear systems. Moreover, whether in continuous or discrete level, the newly reconstructed system still maintains the same energy dissipation law as the original system. On this basis, we establish and analyze the linear unconditionally energy stable schemes from the first- to the fourth-order (in time) based on ESI-SAV approach. As shown in detail, they are high-order accurate (third- and fourth-order in time), easy-to-implement (explicit linear system), and unconditionally energy stable (with a discrete energy dissipation law). In addition, in terms of spatial discretization, we use the second-order central difference formula. Considering the huge computational cost and memory requirement of solving linear systems generated by the nonlocal terms, we choose an efficient computational method [29] based on fast Fourier transform (FFT) and fast conjugate gradient (FCG) approaches to reduce the computational cost.

The structure of this paper is as follows. In section 2, we describe the NCH model with general nonlinear potential and the relationship with the LCH model. In section 3, based on the ESI-SAV approach, we construct the high-order unconditional energy stable schemes for the NCH model. In section 4, we use a variety of the classical numerical examples in 2D to verify the accuracy and efficiency of our proposed schemes.

We use C throughout the paper, with or without subscript, to denote a positive constant, which could have different values at different appearances.

2 The NCH equation

In this section, we will briefly review the NCH equation and the connection with the LCH equation.

2.1 Model formation

The mesoscopic description of phase transition is usually modeled under the assumption that the evolution of order parameter follows the gradient flow of free energy relative to a certain measure. Now let us consider the bounded spatial domain Ω , a rectangular cell in \mathbb{R}^d ($d = 1, 2, 3$). The L^2 inner product and L^2 -norm can be defined as

$$(\phi, \varphi) = \int_{\Omega} \phi(\mathbf{x}) \varphi(\mathbf{x}) d\mathbf{x}, \quad \|\phi\|_2 = (\phi, \phi)^{\frac{1}{2}}, \quad \forall \phi, \varphi \in L^2(\Omega).$$

The general form of the total free energy functional for the NCH equation can be written as [14]:

$$E(\phi) = \int_{\Omega} \left(\frac{\varepsilon^2}{4} \int_{\Omega} J(\mathbf{x} - \mathbf{y}) (\phi(\mathbf{x}) - \phi(\mathbf{y}))^2 d\mathbf{y} + F(\phi(\mathbf{x})) \right) d\mathbf{x}, \quad (1)$$

where ϕ is an order parameter, ε is an interface parameter, which represents the interface thickness and satisfies $0 < \varepsilon \leq 1$, $F(\phi)$ is a nonlinear functional and the most commonly used Ginzburg-Landau double-well potential has the following form:

$$F(\phi) = \frac{(\phi^2 - 1)^2}{4}. \quad (2)$$

Now we introduce the nonlocal diffusion operator \mathcal{L} [14, 20, 21, 29], which is a linear, self-adjoint, positive semi-definite operator:

$$\mathcal{L}\phi = \int_{\Omega} J(\mathbf{x} - \mathbf{y}) (\phi(\mathbf{x}) - \phi(\mathbf{y})) d\mathbf{y}, \quad \mathbf{x} \in \Omega. \quad (3)$$

The interaction kernel J is integrable and satisfies the following conditions [14]:

- (a) $J(\mathbf{x}) \geq 0$ for any $\mathbf{x} \in \Omega$;
- (b) $J(\mathbf{x}) = J(-\mathbf{x})$;
- (c) J is Ω -periodic;
- (d) J is a radial function.

Using the conditions of the kernel J , we get [13]:

$$(\mathcal{L}\phi, \phi) = \frac{1}{2} \int_{\Omega} \int_{\Omega} J(\mathbf{x} - \mathbf{y}) (\phi(\mathbf{x}) - \phi(\mathbf{y}))^2 d\mathbf{y} d\mathbf{x} \geq 0.$$

So the nonlocal total free energy (1) can be written as:

$$E(\phi) = \int_{\Omega} \left(\frac{\varepsilon^2}{2} \phi \mathcal{L}\phi + F(\phi) \right) d\mathbf{x}. \quad (4)$$

2.2 Connection with the LCH equation

We now give a brief introduction to the well-known LCH model [8]. Supposing $\phi(\mathbf{x}, t) : \Omega \times [0, T] \rightarrow [-1, 1]$ is an order parameter, the total free energy takes the form [21]:

$$E_{local}(\phi) = \int_{\Omega} \left(\frac{1}{2} \varepsilon^2 |\nabla \phi|^2 + F(\phi) \right) d\mathbf{x}, \quad (5)$$

where $T > 0$ is the terminal time, $\phi = \pm 1$ corresponds to the steady state of a phase transition.

We can observe that the difference between the LCH equation and the NCH equation is in their free energy. The LCH equation is considered to be derived from the energy functional (5) of the conserved gradient flow:

$$\begin{cases} \frac{\partial \phi}{\partial t} = M \Delta \mu, \\ \mu = -\varepsilon^2 \Delta \phi + f(\phi), \end{cases}$$

where M is the mobility constant, $f(\phi) = F'(\phi)$ is a nonlinear term, and μ is the chemical potential. The unknown $\phi(\mathbf{x}, t)$ is subject to the initial condition $\phi(\mathbf{x}, 0) = \phi_0(\mathbf{x})$, $\mathbf{x} \in \Omega$, with the following boundary condition: periodic, or no flux boundary condition which is given as: $\frac{\partial \phi}{\partial \mathbf{n}} = \frac{\partial \mu}{\partial \mathbf{n}} = 0$ on $\partial\Omega$, where \mathbf{n} is the unit outward normal vector on $\partial\Omega$.

Similarly, using the variational principle for the nonlocal energy functional (4), we can get

$$\begin{cases} \frac{\partial \phi}{\partial t} = M \Delta \mu, \\ \mu = \varepsilon^2 \mathcal{L} \phi + f(\phi). \end{cases} \quad (6)$$

Next, we briefly introduce how the NCH model is derived from the functional variation in the free energy functional (4). Denoting its variational derivative as $\mu = \frac{\delta E}{\delta \phi}$, the general form of the gradient flow model can be written as [38]

$$\frac{\partial \phi}{\partial t} = M \mathcal{G} \mu, \quad (\mathbf{x}, t) \in \Omega \times [0, T] \rightarrow [-1, 1], \quad (7)$$

where the \mathcal{G} is a linear, negative semi-definite operator.

The specific form of the chemical potential μ can be derived by solving the variational derivative of the functional (4), and the process is as follows:

for any function $\eta(\mathbf{x})$, which is sufficiently smooth and satisfies $\eta|_{\partial\Omega} = 0$ on $\partial\Omega$, we have

$$\begin{aligned} \int_{\Omega} \frac{\delta E(\phi)}{\delta \phi} \eta d\mathbf{x} &= \lim_{\theta \rightarrow 0} \frac{E(\phi + \theta \eta) - E(\phi)}{\theta} \\ &= \lim_{\theta \rightarrow 0} \frac{\varepsilon^2}{2\theta} \int_{\Omega} [(\mathcal{L}(\phi + \theta \eta), \phi + \theta \eta) - (\mathcal{L}\phi, \phi)] d\mathbf{x} \\ &\quad + \lim_{\theta \rightarrow 0} \frac{1}{\theta} \int_{\Omega} [F(\phi + \theta \eta) - F(\phi)] d\mathbf{x} \\ &= \varepsilon^2 \int_{\Omega} (\mathcal{L}\phi) \eta d\mathbf{x} + \int_{\Omega} F'(\phi) \eta d\mathbf{x} \\ &= \int_{\Omega} (\varepsilon^2 \mathcal{L}\phi + f(\phi)) \eta d\mathbf{x}, \end{aligned}$$

thus,

$$\mu = \frac{\delta E(\phi)}{\delta \phi} = \varepsilon^2 \mathcal{L}\phi + f(\phi). \quad (8)$$

Then, by combining equations (7), (8), we obtain the NCH model:

$$\begin{cases} \frac{\partial \phi}{\partial t} = M\mathcal{G}\mu, & (\mathbf{x}, t) \in \Omega_T, \\ \mu = \varepsilon^2 \mathcal{L}\phi + f(\phi), & (\mathbf{x}, t) \in \Omega_T, \end{cases} \quad (9)$$

corresponding to initial condition and periodic or no flux boundary conditions. In system (6), we take \mathcal{G} as Δ . If we define \mathcal{G} as the nonlocal diffusion operator $-\mathcal{L}$, we can get a general NCH equation with general nonlinear potential [29]:

$$\begin{cases} \frac{\partial \phi}{\partial t} = -M\mathcal{L}\mu, \\ \mu = \varepsilon^2 \mathcal{L}\phi + f(\phi). \end{cases} \quad (10)$$

Furthermore, in order to explain the relationship between the local and nonlocal energies, we can use Taylor expansion [5, 35] to approximate the interaction energy density with the periodicity of ϕ and J , and the conditions (a) – (d) of J , then we can get

$$\begin{aligned} & \frac{\varepsilon^2}{4} \int_{\Omega} J(\mathbf{x} - \mathbf{y}) (\phi(\mathbf{x}) - \phi(\mathbf{y}))^2 d\mathbf{y} \\ &= \frac{\varepsilon^2}{4} \int_{\Omega} J(\mathbf{y}) (\phi(\mathbf{x}) - \phi(\mathbf{x} + \mathbf{y}))^2 d\mathbf{y} \\ &\approx \frac{\varepsilon^2}{4} \int_{\Omega} J(\mathbf{y}) |\mathbf{y}|^2 |\nabla \phi(\mathbf{x})|^2 d\mathbf{y} \\ &= \frac{\varepsilon^2}{2} |\nabla \phi(\mathbf{x})|^2. \end{aligned}$$

The operator $-\mathcal{L}$ of the NCH model (10) is negative semi-definite, so the free energy equation (4) is decreasing with time,

$$\begin{aligned} \frac{dE(\phi(t))}{dt} &= \frac{d}{dt} \left(\frac{\varepsilon^2}{2} (\mathcal{L}\phi, \phi) + \int_{\Omega} F(\phi) d\mathbf{x} \right) \\ &= (\phi_t, \varepsilon^2 \mathcal{L}\phi) + (\phi_t, f(\phi)) \\ &= (\phi_t, \varepsilon^2 \mathcal{L}\phi + f(\phi)) \\ &= (-M\mathcal{L}\mu, \mu) \leq 0. \end{aligned} \quad (11)$$

3 The ESI-SAV scheme for the NCH equation

In this section, we will construct and analyze the linear high-order semi-discrete time marching numerical schemes for the NCH model with general nonlinear potential. It will be clear that the unconditional energy stability of the semi-discrete scheme is also valid in the fully discrete formulation. Let $N_t > 0$ be a positive integer, and

$$T = N_t \Delta t, \quad t^n = n \Delta t, \quad \forall n \leq N_t.$$

For the ESI-SAV approach, similar to [30], we introduce an exponential scalar auxiliary variable :

$$R(t) = \exp(E(\phi)) = \exp \left(\frac{\varepsilon^2}{2} (\mathcal{L}\phi, \phi) + \int_{\Omega} F(\phi) d\mathbf{x} \right) > 0, \quad \forall t \in [0, T].$$

Then the equivalent new format of the NCH model (10) is:

$$\begin{cases} \frac{\partial \phi}{\partial t} = -M\mathcal{L}\mu, \\ \mu = \varepsilon^2 \mathcal{L}\phi + \frac{R}{\exp(E(\phi))} f(\phi), \\ \frac{dR}{dt} = R(-M\mathcal{L}\mu, \mu). \end{cases} \quad (12)$$

For the above system, the new energy is defined as $\ln R$, and it can be observed that the new energy is equivalent to the original energy, that is $\ln R = E$, and satisfies the energy dissipation law. Rewrite the third equation of the above system (12), we get

$$\frac{dE}{dt} = \frac{d \ln R}{dt} = \frac{1}{R} \frac{dR}{dt} = (-M\mathcal{L}\mu, \mu) \leq 0.$$

This result is consistent with the energy dissipation law of the original energy (11).

3.1 First-order ESI-SAV scheme

The first-order ESI-SAV scheme for (12) reads as:

$$\begin{cases} \frac{\phi^{n+1} - \phi^n}{\Delta t} = -M\mathcal{L}\mu^{n+1}, \\ \mu^{n+1} = \varepsilon^2 \mathcal{L}\phi^{n+1} + \frac{R^{n+1}}{\exp(E(\phi^n))} f(\phi^n), \\ \frac{R^{n+1} - R^n}{\Delta t} = R^{n+1}(-M\mathcal{L}\bar{\mu}^n, \bar{\mu}^n), \end{cases} \quad (13)$$

with the initial conditions

$$\begin{aligned} \phi^0 &= \phi_0(\mathbf{x}), \quad \forall \mathbf{x} \in \Omega, \\ R^0 &= \exp(E(\phi^0)). \end{aligned}$$

Theorem 3.1 *The scheme (13) for the NCH equation is unconditionally energy stable in the sense that*

$$R^{n+1} - R^n = -R^{n+1} \Delta t (M\mathcal{L}\bar{\mu}^n, \bar{\mu}^n) \leq 0,$$

and more importantly we have

$$\ln R^{n+1} - \ln R^n \leq 0.$$

Proof: By the definition of $R(t)$ and the negative semi-definite operator $-\mathcal{L}$, we obtain $R^{n+1} = \frac{R^n}{1 + \Delta t (M\mathcal{L}\bar{\mu}^n, \bar{\mu}^n)} > 0$. Then combining the inequality $R^{n+1} > 0$ with the third equation of (13), we can easily obtain the following modified energy stability:

$$R^{n+1} - R^n = R^{n+1} \Delta t M(\mathcal{G}\bar{\mu}^n, \bar{\mu}^n) \leq 0.$$

Noting that $E(\phi) = \ln(\exp(E(\phi))) = \ln R$ and the logarithm function is strictly monotonically increasing, we can also obtain the following energy stability:

$$\ln R^{n+1} - \ln R^n \leq 0.$$

□

Next, in order to show the computational simplicity and effectiveness of the proposed numerical scheme, we give the explicit process for solving the first-order scheme (13) as below, and other high-order schemes are solved similarly. By rewriting the scheme (13), we can get

$$\left(\frac{1}{\Delta t} + M\varepsilon^2\mathcal{L}^2\right)\phi^{n+1} = \frac{1}{\Delta t}\phi^n - M\mathcal{L}\frac{R^{n+1}}{\exp(E(\phi^n))}f(\phi^n), \quad (14a)$$

$$R^{n+1} = \frac{R^n}{1 + \Delta t(M\mathcal{L}\bar{\mu}^n, \bar{\mu}^n)}. \quad (14b)$$

Obviously, (14) is uniquely solvable for any $\Delta t > 0$ since $\frac{1}{\Delta t} + M\varepsilon^2\mathcal{L}^2$ is positive definite. To summarize, we implement (13) as follows:
with the value of ϕ^n known,

- (i) Compute $\bar{\mu}^n$ by $\bar{\mu}^n = \varepsilon^2\mathcal{L}\phi^n + f(\phi^n)$,
- (ii) Compute R^{n+1} from equation (14b),
- (iii) Compute ϕ^{n+1} from equation (14a).

Note that in the above steps (ii), (iii), we only need to solve explicitly two linear equations with constant coefficients of the form

$$\bar{A}\bar{\phi} = \bar{b}.$$

3.2 Second-order Crank-Nicolson scheme

In this section, we will present and analyze linear, second-order (in time) numerical ESI-SAV scheme based on the Crank-Nicolson formula. We firstly introduce a new variable $\xi = \frac{R}{\exp(E(\phi))}$. It is obviously that $\xi \equiv 1$ at the continuous level, and $\xi(2 - \xi)$ is also equal to 1. So the system (10) can be rewritten as:

$$\left\{ \begin{array}{l} \frac{\partial \phi}{\partial t} = -M\mathcal{L}\mu, \\ \mu = \varepsilon^2\mathcal{L}\phi + \xi(2 - \xi)f(\phi), \\ \xi = \frac{R}{\exp(E(\phi))}, \\ \frac{dR}{dt} = R(-M\mathcal{L}\mu, \mu). \end{array} \right. \quad (15)$$

The new equivalent system also maintains the original energy dissipation law:

$$\frac{dE}{dt} = \frac{d(\ln R)}{dt} = \frac{1}{R} \frac{dR}{dt} = (-M\mathcal{L}\mu, \mu) \leq 0.$$

A second-order ESI-SAV scheme for the system (15) reads as:

$$\left\{ \begin{array}{l} \frac{\phi^{n+1} - \phi^n}{\Delta t} = -M\mathcal{L}\mu^{n+\frac{1}{2}}, \\ \mu^{n+\frac{1}{2}} = \varepsilon^2 \mathcal{L} \frac{\phi^{n+1} + \phi^n}{2} + V(\xi^{n+1}) f(\phi^{*,n+\frac{1}{2}}), \\ \xi^{n+1} = \frac{R^{n+1}}{\exp(E(\phi^{*,n+\frac{1}{2}}))}, \\ V(\xi^{n+1}) = \xi^{n+1} (2 - \xi^{n+1}), \\ \frac{R^{n+1} - R^n}{\Delta t} = R^{n+1} (-M\mathcal{L}\bar{\mu}^{n+\frac{1}{2}}, \bar{\mu}^{n+\frac{1}{2}}), \end{array} \right. \quad (16)$$

with the initial conditions

$$\begin{aligned} \phi^0 &= \phi_0(\mathbf{x}), \quad \forall \mathbf{x} \in \Omega, \\ R^0 &= \exp(E(\phi^0)), \end{aligned}$$

where $\bar{\mu}^{n+\frac{1}{2}} = \varepsilon^2 \mathcal{L}\phi^{*,n+\frac{1}{2}} + f(\phi^{*,n+\frac{1}{2}})$, $\phi^{*,n+\frac{1}{2}}$ is any explicit $O(\Delta t^2)$ approximation of $\phi(t^{n+\frac{1}{2}})$. We can choose the extrapolation formula

$$\phi^{*,n+\frac{1}{2}} = \frac{3}{2}\phi^n - \frac{1}{2}\phi^{n-1}, \quad n \geq 1,$$

and for $\phi^{*,\frac{1}{2}}$, we can obtain it as follows:

$$\frac{\phi^{*,\frac{1}{2}} - \phi^0}{\Delta t/2} = -M\mathcal{L}(\varepsilon^2 \mathcal{L}\phi^{*,\frac{1}{2}} + f(\phi^0)).$$

Similar to the proof of Theorem 3.1, we can easily get the following theorem:

Theorem 3.2 *The scheme (16) for the NCH equation is unconditionally energy stable in the sense that*

$$R^{n+1} - R^n = R^{n+1} \Delta t (-M\mathcal{L}\bar{\mu}^{n+\frac{1}{2}}, \bar{\mu}^{n+\frac{1}{2}}) \leq 0, \quad (17)$$

and more importantly we have

$$\ln R^{n+1} - \ln R^n \leq 0. \quad (18)$$

3.3 High-order BDF k schemes

We use the ESI-SAV method combined with k -step BDF (BDF k) to extend the high-order unconditional energy stability scheme for the NCH equation. Now firstly we rewrite the system (10) by introducing a new function $V(\xi)$ which is equal to 1 at the continuous level:

$$\left\{ \begin{array}{l} \frac{\partial \phi}{\partial t} = -M\mathcal{L}\mu, \\ \mu = \varepsilon^2 \mathcal{L}\phi + V(\xi) f(\phi), \\ \xi = \frac{R}{\exp(E(\phi))}, \\ \frac{dR}{dt} = R(-M\mathcal{L}\mu, \mu). \end{array} \right. \quad (19)$$

The new equivalent system also keeps the original energy dissipation law:

$$\frac{dE}{dt} = \frac{d \ln(R)}{dt} = \frac{1}{R} \frac{dR}{dt} = (-M\mathcal{L}\mu, \mu) \leq 0.$$

Denoting $V(\xi) = \xi(2 - \xi)$, a second-order ESI-SAV scheme based on the BDF2 formula for (19) reads as:
for $n \geq 1$,

$$\begin{cases} \frac{3\phi^{n+1} - 4\phi^n + \phi^{n-1}}{2\Delta t} = -M\mathcal{L}\mu^{n+1}, \\ \mu^{n+1} = \varepsilon^2 \mathcal{L}\phi^{n+1} + V(\xi^{n+1}) f(\phi^{*,n+1}), \\ V(\xi^{n+1}) = \xi^{n+1}(2 - \xi^{n+1}), \\ \xi^{n+1} = \frac{R^{n+1}}{\exp(E(\phi^{*,n+1}))}, \\ \frac{R^{n+1} - R^n}{\Delta t} = R^{n+1}(-M\mathcal{L}\bar{\mu}^{n+1}, \bar{\mu}^{n+1}), \end{cases} \quad (20)$$

with the initial conditions

$$\begin{aligned} \phi^0 &= \phi_0(\mathbf{x}), \quad \forall \mathbf{x} \in \Omega, \\ R^0 &= \exp(E(\phi^0)), \end{aligned}$$

where $\bar{\mu}^{n+1} = \varepsilon^2 \mathcal{L}\phi^{*,n+1} + f(\phi^{*,n+1})$, $\phi^{*,n+1}$ is any explicit $O(\Delta t^2)$ approximation of $\phi(t^{n+1})$, so it can be calculated by

$$\phi^{*,n+1} = 2\phi^n - \phi^{n-1}, \quad n \geq 1.$$

Denoting $V(\xi) = \xi(3 - 3\xi + \xi^2)$, a third-order ESI-SAV scheme based on the BDF3 formula for (19) reads as:
for $n \geq 2$,

$$\begin{cases} \frac{11\phi^{n+1} - 18\phi^n + 9\phi^{n-1} - 2\phi^{n-2}}{6\Delta t} = -M\mathcal{L}\mu^{n+1}, \\ \mu^{n+1} = \varepsilon^2 \mathcal{L}\phi^{n+1} + V(\xi^{n+1}) f(\phi^{*,n+1}), \\ V(\xi^{n+1}) = \xi^{n+1}(3 - 3\xi^{n+1} + (\xi^{n+1})^2), \\ \xi^{n+1} = \frac{R^{n+1}}{\exp(E(\phi^{*,n+1}))}, \\ \frac{R^{n+1} - R^n}{\Delta t} = R^{n+1}(-M\mathcal{L}\bar{\mu}^{n+1}, \bar{\mu}^{n+1}), \end{cases} \quad (21)$$

where $\bar{\mu}^{n+1} = \varepsilon^2 \mathcal{L}\phi^{*,n+1} + f(\phi^{*,n+1})$, $\phi^{*,n+1}$ is any explicit $O(\Delta t^3)$ approximation of $\phi(t^{n+1})$, and can be calculated by

$$\phi^{*,n+1} = 3\phi^n - 3\phi^{n-1} + \phi^{n-2}, \quad n \geq 2.$$

Denoting $V(\xi) = \xi(2 - \xi)(2 - 2\xi + \xi^2)$, a fourth-order ESI-SAV scheme based on the BDF4 formula for (19) reads as:

for $n \geq 3$,

$$\left\{ \begin{array}{l} \frac{25\phi^{n+1} - 48\phi^n + 36\phi^{n-1} - 16\phi^{n-2} + 3\phi^{n-3}}{12\Delta t} = -M\mathcal{L}\mu^{n+1}, \\ \mu^{n+1} = \varepsilon^2 \mathcal{L}\phi^{n+1} + V(\xi^{n+1}) f(\phi^{*,n+1}), \\ V(\xi^{n+1}) = \xi^{n+1} (2 - \xi^{n+1}) (2 - 2\xi^{n+1} + (\xi^{n+1})^2), \\ \xi^{n+1} = \frac{R^{n+1}}{\exp(E(\phi^{*,n+1}))}, \\ \frac{R^{n+1} - R^n}{\Delta t} = R^{n+1} (-M\mathcal{L}\bar{\mu}^{n+1}, \bar{\mu}^{n+1}), \end{array} \right. \quad (22)$$

where $\bar{\mu}^{n+1} = \varepsilon^2 \mathcal{L}\phi^{*,n+1} + f(\phi^{*,n+1})$, $\phi^{*,n+1}$ is any explicit $O(\Delta t^4)$ approximation of $\phi(t^{n+1})$, and can be calculated by

$$\phi^{*,n+1} = 4\phi^n - 6\phi^{n-1} + 4\phi^{n-2} - \phi^{n-3}, \quad n \geq 3.$$

Similar to the proof of Theorem 3.1, we can easily get the following theorem:

Theorem 3.3 *The schemes (20)-(22) for the NCH equation is unconditionally energy stable in the sense that*

$$R^{n+1} - R^n = R^{n+1} \Delta t (-M\mathcal{L}\bar{\mu}^{n+1}, \bar{\mu}^{n+1}) \leq 0,$$

and more importantly we have

$$\ln R^{n+1} - \ln R^n \leq 0.$$

3.4 The improvement of the schemes

In order to prevent the instability of the result caused by the rapid growth of the exponential function, and ensure the energy dissipation law, we can add a positive number C large enough to redefine the exponential scalar auxiliary variable:

$$R(t) = \exp\left(\frac{E(\phi)}{C}\right) = \exp\left(\frac{\varepsilon^2}{2C} (\mathcal{L}\phi, \phi) + \frac{1}{C} \int_{\Omega} F(\phi) d\mathbf{x}\right). \quad (23)$$

Then the scheme (19) can be improved to the following equivalent format:

$$\left\{ \begin{array}{l} \frac{\partial \phi}{\partial t} = -M\mathcal{L}\mu, \\ \mu = \varepsilon^2 \mathcal{L}\phi + V(\xi) f(\phi), \\ \xi = \frac{R}{\exp\left(\frac{E(\phi)}{C}\right)}, \\ \frac{dR}{dt} = \frac{R}{C} (-M\mathcal{L}\mu, \mu). \end{array} \right.$$

According to formula (23), the modified free energy can be defined as $C \ln R$, furthermore, it satisfies $C \ln R = E$ at the continuous level. The new equivalent system also keeps the original energy dissipation law:

$$\frac{dE}{dt} = \frac{d(C \ln R)}{dt} = \frac{C}{R} \frac{dR}{dt} = -M(\mathcal{L}\mu, \mu) \leq 0.$$

3.5 Spatial discretization

We use the second-order central finite difference formula to discretize the spatial operator. Let N_x, N_y be positive integers and the two dimensional domain $\Omega = [-L_x, L_x] \times [-L_y, L_y]$. For simplicity of explanation, we consider periodic boundary conditions for the NCH equation. We divide the domain into rectangular meshes with mesh size

$$h_x = \frac{2L_x}{N_x}, h_y = \frac{2L_y}{N_y}.$$

So we define the following uniform grid:

$$\Omega_h = \{(x_i, y_j) \mid x_i = -L_x + ih_x, y_j = -L_y + jh_y, 0 \leq i \leq N_x, 0 \leq j \leq N_y\}.$$

From [14, 30], we can write the nonlocal operator \mathcal{L} in (3) as the following equivalent form:

$$\mathcal{L}\phi = (J * 1)\phi - J * \phi,$$

where

$$\begin{aligned} J * 1 &= \int_{\Omega} J(\mathbf{x}) d\mathbf{x}, \\ (J * \phi)(\mathbf{x}) &= \int_{\Omega} J(\mathbf{x} - \mathbf{y})\phi(\mathbf{y}) d\mathbf{y} = \int_{\Omega} J(\mathbf{y})\phi(\mathbf{x} - \mathbf{y}) d\mathbf{y}, \end{aligned}$$

are exactly the periodic convolutions.

For any ϕ , we can discrete $\mathcal{L}\phi$ at $(t^n, x_i, y_j), (x_i, y_j) \in \Omega_h$, as follows:

$$(\mathcal{L}_h \phi)_{i,j}^n = (J * 1)_{i,j} \phi_{i,j}^n - (J * \phi)_{i,j}^n, \quad (24)$$

where

$$\begin{aligned} (J * 1)_{i,j} \phi_{i,j}^n &= h_x h_y \left[\sum_{m_1=1}^{N_x-1} \sum_{m_2=1}^{N_y-1} J(x_{m_1} - x_i, y_{m_2} - y_j) \right. \\ &\quad + \frac{1}{2} \sum_{m_1=1}^{N_x-1} (J(x_{m_1} - x_i, y_0 - y_j) + J(x_{m_1} - x_i, y_{N_y} - y_j)) \\ &\quad + \frac{1}{2} \sum_{m_2=1}^{N_y-1} (J(x_0 - x_i, y_{m_2} - y_j) + J(x_{N_x} - x_i, y_{m_2} - y_j)) \\ &\quad + \frac{1}{4} (J(x_0 - x_i, y_0 - y_j) + J(x_{N_x} - x_i, y_0 - y_j)) \\ &\quad \left. + \frac{1}{4} (J(x_0 - x_i, y_{N_y} - y_j) + J(x_{N_x} - x_i, y_{N_y} - y_j)) \right] \phi_{i,j}^n, \end{aligned}$$

and

$$\begin{aligned}
(J * \phi)_{i,j}^n = & h_x h_y \left[\sum_{m_1=1}^{N_x-1} \sum_{m_2=1}^{N_y-1} J(x_{m_1} - x_i, y_{m_2} - y_j) \phi_{m_1, m_2}^n \right. \\
& + \frac{1}{2} \sum_{m_1=1}^{N_x-1} \left(J(x_{m_1} - x_i, y_0 - y_j) \phi_{m_1, 0}^n + J(x_{m_1} - x_i, y_{N_y} - y_j) \phi_{m_1, N_y}^n \right) \\
& + \frac{1}{2} \sum_{m_2=1}^{N_y-1} \left(J(x_0 - x_i, y_{m_2} - y_j) \phi_{0, m_2}^n + J(x_{N_x} - x_i, y_{m_2} - y_j) \phi_{N_x, m_2}^n \right) \\
& + \frac{1}{4} \left(J(x_0 - x_i, y_0 - y_j) \phi_{0, 0}^n + J(x_{N_x} - x_i, y_0 - y_j) \phi_{N_x, 0}^n \right) \\
& \left. + \frac{1}{4} \left(J(x_0 - x_i, y_{N_y} - y_j) \phi_{0, N_y}^n + J(x_{N_x} - x_i, y_{N_y} - y_j) \phi_{N_x, N_y}^n \right) \right].
\end{aligned}$$

Combining the fourth-order system (22), and the discrete nonlocal operator expression (24), we obtain the corresponding fully discrete finite difference scheme as follows:

$$\left\{ \begin{array}{l} \frac{25\phi_{i,j}^{n+1} - 48\phi_{i,j}^n + 36\phi_{i,j}^{n-1} - 16\phi_{i,j}^{n-2} + 3\phi_{i,j}^{n-3}}{\Delta t} = -M(\mathcal{L}_h \mu)_{i,j}^{n+1}, \\ \mu_{i,j}^{n+1} = \varepsilon^2 (\mathcal{L}_h \phi)_{i,j}^{n+1} + V(\xi^{n+1}) f(\phi_{i,j}^{*,n+1}), \\ V(\xi^{n+1}) = \xi^{n+1} (2 - \xi^{n+1}) (2 - 2\xi^{n+1} + (\xi^{n+1})^2), \\ \xi^{n+1} = \frac{R^{n+1}}{\exp(E(\phi^{*,n+1}))}, \\ \frac{R^{n+1} - R^n}{\Delta t} = R^{n+1} \sum_{i=0}^{N_x} \sum_{j=0}^{N_y} M(\mathcal{G}_h \bar{\mu})_{i,j}^{n+1} \bar{\mu}_{i,j}^{n+1}, \end{array} \right. \quad (25)$$

where

$$\begin{aligned}
\bar{\mu}_{i,j}^{n+1} &= \varepsilon^2 (\mathcal{L}_h \phi)_{i,j}^{*,n+1} + f(\phi_{i,j}^{*,n+1}), \quad n \geq 3, 0 \leq i \leq N_x, 0 \leq j \leq N_y, \\
\phi_{i,j}^{*,n+1} &= 4\phi_{i,j}^n - 6\phi_{i,j}^{n-1} + 4\phi_{i,j}^{n-2} - \phi_{i,j}^{n-3}, \quad n \geq 3, 0 \leq i \leq N_x, 0 \leq j \leq N_y.
\end{aligned}$$

In order to monitor the change of free energy during evolution, the original discrete energy functional is defined as:

$$E^n = \sum_{i=0}^{N_x} \sum_{j=0}^{N_y} F(\phi_{i,j}^n) + \frac{\varepsilon^2}{2} \sum_{i=0}^{N_x} \sum_{j=0}^{N_y} (\mathcal{L}_h \phi)_{i,j}^n \cdot \phi_{i,j}^n. \quad (26)$$

In addition, combined with the R^n of scheme (25), the modified discrete energy functional can be defined as:

$$\bar{E}^n = C \ln(R^n). \quad (27)$$

We can see that the nonlocal diffusion term will lead the stiffness maxtrix to be almost full matrix which requires huge computational work and large memory. In this case, the fast solution method for solving the derived linear system will become very important and necessary. Due to the special

structure of coefficient matrices, we adopt the similar methods as [29] to ensure the efficiency of the algorithm based on the Fast Fourier transform (FFT) and the fast conjugate gradient (FCG) method. We set $N_x = N_y = N$, the overall computational cost of the FCG method is $O(N \log^2 N)$ with the number of iterations $O(\log N)$, instead of $O(N^3)$ by using the Gaussian elimination method, and the fast solver will reduce memory requirement from $O(N^2)$ to $O(N)$.

4 Numerical simulations

In this section, various simulations are provided to verify the theoretical results of the developed numerical schemes.

This smooth kernel is given by the Gaussian function in the following form [14]:

$$J_\delta = \frac{4}{\pi^{d/2} \delta^{d+2}} e^{-\frac{|\mathbf{x}|^2}{\delta^2}}, \quad \mathbf{x} \in \Omega \subset \mathbb{R}^d, \quad \delta > 0, \quad (28)$$

and it satisfies

$$\begin{aligned} \int_{\mathbb{R}^d} J_\delta(\mathbf{x}) d\mathbf{x} &= \frac{4}{\delta^2}, \\ \int_{\mathbb{R}^d} J_\delta(\mathbf{x}) |\mathbf{x}| d\mathbf{x} &= 2d. \end{aligned}$$

From [14], this kernel J_δ has the proposition: for any $\phi \in C^\infty(\Omega)$, $\mathbf{x} \in \Omega$, $\mathcal{L}_\delta \phi(\mathbf{x}) \rightarrow -\Delta \phi(\mathbf{x})$, as $\delta \rightarrow 0$. It tells us that the NCH equation with Gaussian kernel converges to the LCH equation when δ approaches zero. Using the nonlocal kernel J_δ with $\delta = \sqrt{0.1}$, $d = 2$, we show its profile projection in 2D by figure 1.

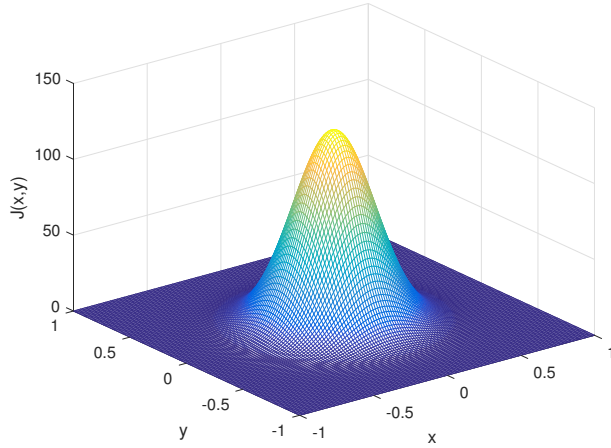


Figure 1: The profile of nonlocal kernel J_δ defined in (28)

In the following numerical examples, we choose some numerical simulations in two dimension to verify the unconditional energy stability and temporal convergence rate. We specify the rectangular domain as $\Omega = [-1, 1] \times [-1, 1]$, and the finite difference scheme is used in space, where $N = 100$.

Note that we denote the first-order ESI-SAV scheme (13) by BDF1, the second-order ESI-SAV scheme based on the Crank-Nicolson formula (16) by CN, the high-order ESI-SAV schemes based on BDFk formula (20), (21), (22) by BDFk (k=2,3,4). In order to verify the effectiveness of the fast solver (i.e. using FTT and FCG algorithm), we compare them with the CPU time for the direct solver (i.e. solving with $\bar{\phi} = \bar{A}^{-1}\bar{b}$), and abbreviate the fast solver and the direct solver as FS and DS respectively.

In our practical calculation, we will specify the operator \mathcal{L} , the bulk potential $F(\phi)$ as $\bar{\mathcal{L}}, \bar{F}(\phi)$ respectively:

$$\begin{aligned}\bar{\mathcal{L}} &= \mathcal{L} + \frac{\beta}{\varepsilon^2}, \\ \bar{F}(\phi) &= \frac{1}{4}(\phi^2 - 1 - \beta)^2,\end{aligned}$$

where $\beta > 0$ is a suitable parameter to ensure sufficient dissipation of the implicit part of the numerical scheme [14]. In the following numerical examples, when the error of the absolute value of the energy at two consecutive moments is less than the tolerance value of $1e-8$, we consider that the phase transition process has reached a steady state.

Example 1 For the first numerical example, we consider the NCH equation equipped with the Gaussian kernel J_δ and the required parameters are $M = 1, \varepsilon^2 = 0.1, \delta = \varepsilon, T = 0.05$. In order to perform the refinement test of the time step, we use a linear refinement path in time: $\Delta t = T/T_n, T_n = 2^n, n = 3, 4, \dots, 10$, Δt is the time step. One thing to notice is that we have no exact solution to compare, then we choose the difference between the results on continuous coarse grid and fine grid as the error calculation. That is, by taking the linear refinement path, we calculate the convergence rate by Cauchy error, e.g. $\|\phi^{n+1} - \phi^n\|_2$. Now we give the following initial condition:

$$\phi_0(x, y) = 0.8 \sin(\pi x) \sin(\pi y).$$

The comparison between the fast solver (FS) and the direct solver (DS) is shown in Table 1 and Table 2, where the time is in seconds. It can be seen that the fast solver reduces the CPU time and greatly improves the computational efficiency. Table 3 shows the L^2 -norm errors and temporal convergence rates of the schemes proposed in the previous section. As the time step decreases, the convergence rate gets closer to the optimal order of convergence.

Example 2 For the second numerical example, we choose the benchmark problem [29] governed by the NCH equation equipped with the Gaussian kernel J_δ , and the initial condition is

$$\phi_0(x, y) = \sum_{i=1}^2 -\tanh\left(\frac{\sqrt{(x-a_i)^2 + (y-b_i)^2} - R_0}{\sqrt{2}\varepsilon}\right).$$

In addition, we need to know some parameters, the radius $R_0 = 0.36$, the two bubble centers $(a_1, b_1) = (0.4, 0)$ and $(a_2, b_2) = (-0.4, 0)$. We adopt the third order ESI-SAV BDF3 scheme for this example. The required parameters are $\varepsilon = 0.02, \delta = \varepsilon, \Delta t = 1e-3$.

The evolution of the phase field variable ϕ at $t = 0, 0.1, 0.6, 1, 5, 10$ are shown in Figure 2. From the snapshots, we observe that the two bubbles are just close to each other initially. With the time evolution, the two bubbles fuse with each other, which can also be said that the small bubble is absorbed by the large bubble. Moreover, due to the mass conservation of phase field variables in the NCH model, the two small bubbles will turn into a large round bubble. After $t = 11$, they tend to a stable phase state, that is, there is only one large bubble. The result is consistent with that in [29].

Table 1: The CUP time(s) for direct solver (DS) and fast solver (FS) which are used for **Example 1** by the first-order BDF1 scheme

T_n	2^3	2^4	2^5	2^6	2^7	2^8	2^9
DS	212.69	213.19	397.17	756.74	1430.69	2794.43	5547.35
FS	3.99	6.10	6.39	10.68	18.40	32.22	56.31

Table 2: The CUP time(s) for direct solver (DS) and fast solver(FS) which are used for **Example 1** by the second-order CN scheme

T_n	2^3	2^4	2^5	2^6	2^7	2^8	2^9
DS	132.44	230.01	421.47	779.01	1519.85	3001.38	5954.90
FS	2.88	4.05	6.58	11.13	18.55	32.10	57.36

Table 3: the L^2 errors and temporal convergence rates of the five schemes for the **Example 1**

	T_n	2^3	2^4	2^5	2^6	2^7	2^8
BDF1	Error	1.16e-2	6.35e-3	3.32e-3	1.70e-3	8.60e-4	4.32e-4
	Rate	—	0.8686	0.9341	0.9672	0.9836	0.9918
CN	Error	1.79e-3	4.69e-4	1.21e-4	3.07e-5	7.76e-6	1.95e-6
	Rate	—	1.9326	1.9551	1.9748	1.9868	1.9932
BDF2	Error	1.85e-2	5.15e-3	1.35e-3	3.48e-4	8.80e-5	2.22e-5
	Rate	—	1.8453	1.9257	1.9626	1.9811	1.9906
BDF3	Error	7.69e-3	1.08e-3	1.45e-4	1.88e-5	2.40e-6	3.03e-7
	Rate	—	2.8275	2.9030	2.9451	2.9704	2.9846
BDF4	Error	9.40e-4	7.71e-5	5.47e-6	3.62e-7	2.33e-8	1.47e-9
	Rate	—	3.6075	3.8174	3.9167	3.9608	3.9810

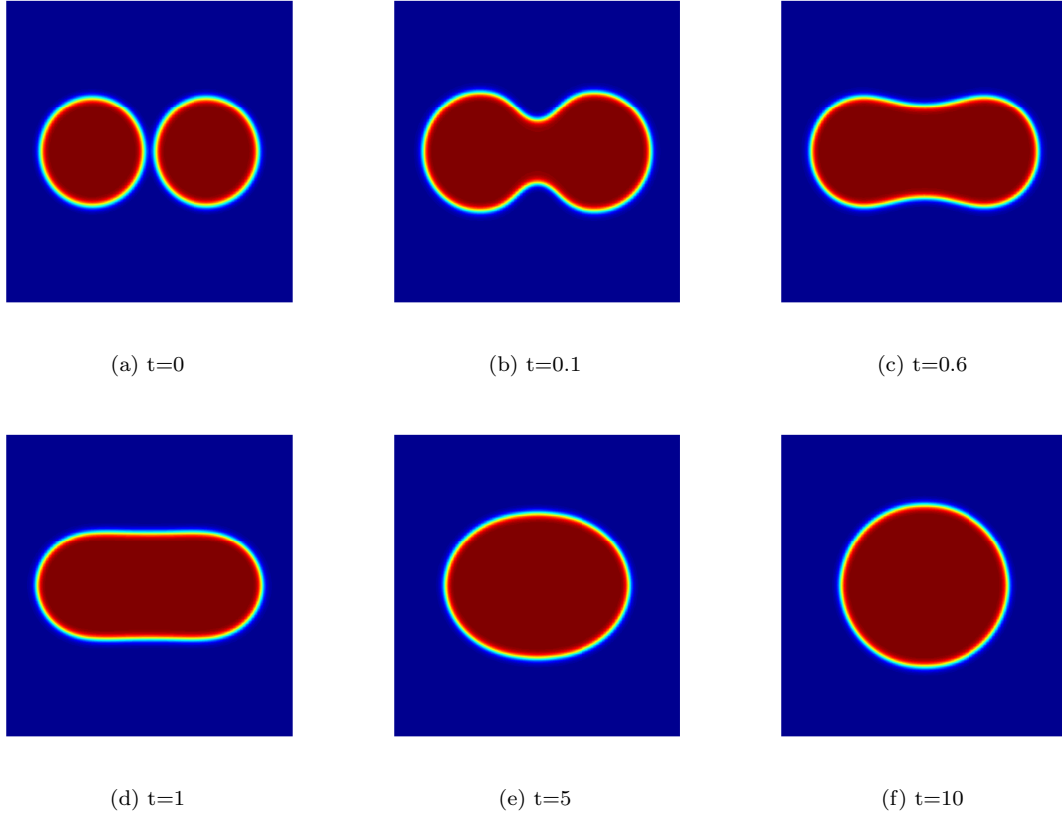


Figure 2: Snapshots of the phase variable ϕ are taken at $t = 0, 0.1, 0.6, 1, 5, 10$ for **Example 2**

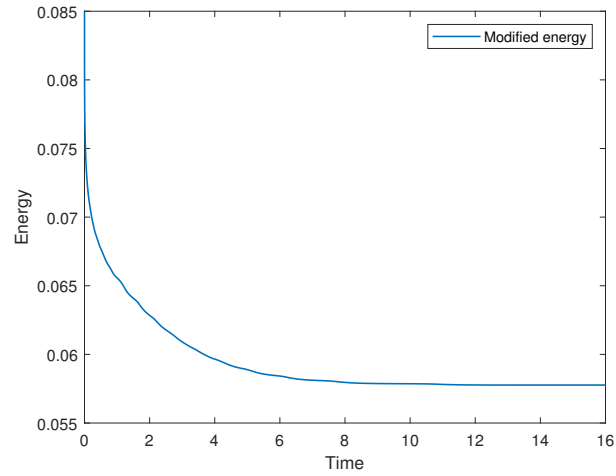


Figure 3: Time evolution of the modified discrete free energy functional (27) for **Example 2**

In Figure 3, we draw the evolution of the energy curve, which verifies that the modified discrete energy does conform to the law of energy dissipation law.

Example 3 In this example, we study the coarsening dynamic model driven by the NCH equation. We still use the same kernel function specified in (28) to simulate the long time behavior of the phase transition. We set the initial conditions as the randomly perturbed concentration field as shown below:

$$\phi_0(x, y) = \phi_a + \phi_b \text{rand}(x, y),$$

where $\text{rand}(x, y)$ is the random number in $[-1, 1]$ with zero mean.

The other required parameters are shown in Table 4.

Table 4: The required parameters in **Example 3**

ε	δ	Δt
0.02	0.02	$1e-3$

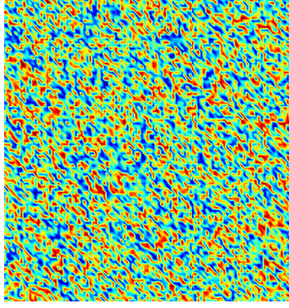
The long-time coarsening dynamical behaviors of the phase separation are shown in Figure 4 and Figure 5. The snapshots are taken at $t = 0, 0.2, 1, 8, 15$, and the time of final steady state. We adjust the values of ϕ_a and ϕ_b to obtain various coarsening dynamics model. In Figure 4, we perform numerical simulations for initial values with $\phi_a = 0, \phi_b = 0.1$, and we observe that the final equilibrium solution after $t = 39$ shows a red circle. In Figure 5, we choose $\phi_a = 0.1$ and $\phi_b = 0.001$, the final equilibrium solution after $t = 33$ shows a blue circle, but the value of ϕ in the circle becomes the exact opposite of that in Figure 4. The results is consistent with that in [29, 43]. In Figure 6, we can see that the original discrete energy decreases over time, which satisfies the energy dissipation law.

5 Conclusion

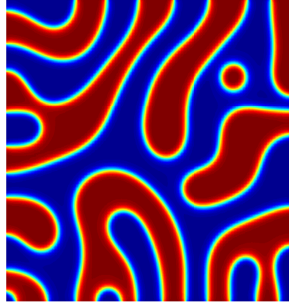
In this paper, we construct the high-order and effective linear schemes based on the ESI-SAV for solving the NCH equation with general nonlinear potential. Through the comparison of the LCH and NCH models, we analyze the nonlocal model and related properties. We focus on the method of numerical discretization with high-order accuracy (in time) of the NCH model and use the ESI-SAV method to deal with nonlocal diffusion term implicitly and nonlinear term explicitly by introducing a scalar auxiliary variable. Under the assumption of positive kernel, we prove the unconditional energy stability of the semi-discrete scheme carefully and rigorously. Furthermore, the discrete energy dissipation law of the proposed numerical schemes is guaranteed. In addition, we consider integrable kernel only to make the calculation simple. Due to the properties of Gaussian kernel parameterized by δ of nonlocal operator and the special format of coefficient matrix, we can use a fast solver based on FFT and FCG to reduce the amount of storage and computation cost required in fully discrete format, which does greatly shorten the CPU time. Finally, we demonstrate the effectiveness, accuracy and unconditional energy stability of the proposed numerical scheme by using different classical numerical experiments.

Acknowledgement

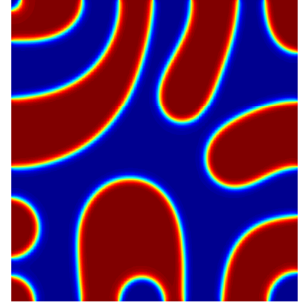
This work was supported in part by the National Natural Science Foundation of China under Grants 11971272, 12001336.



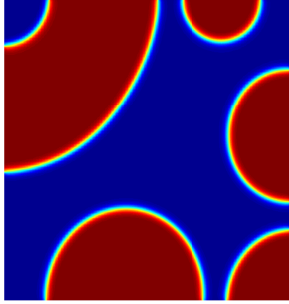
(a) $t=0$



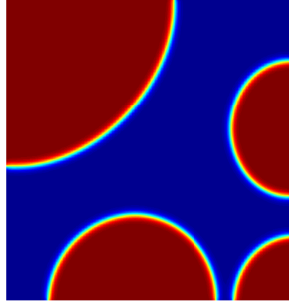
(b) $t=0.2$



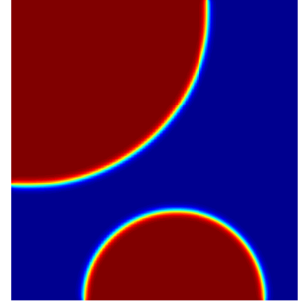
(c) $t=1$



(d) $t=8$



(e) $t=15$



(f) $t=39$

Figure 4: Snapshots of the phase variable ϕ at $t = 0, 0.2, 1, 8, 15, 39$ with $\phi_a = 0, \phi_b = 0.1$ for **Example 3**

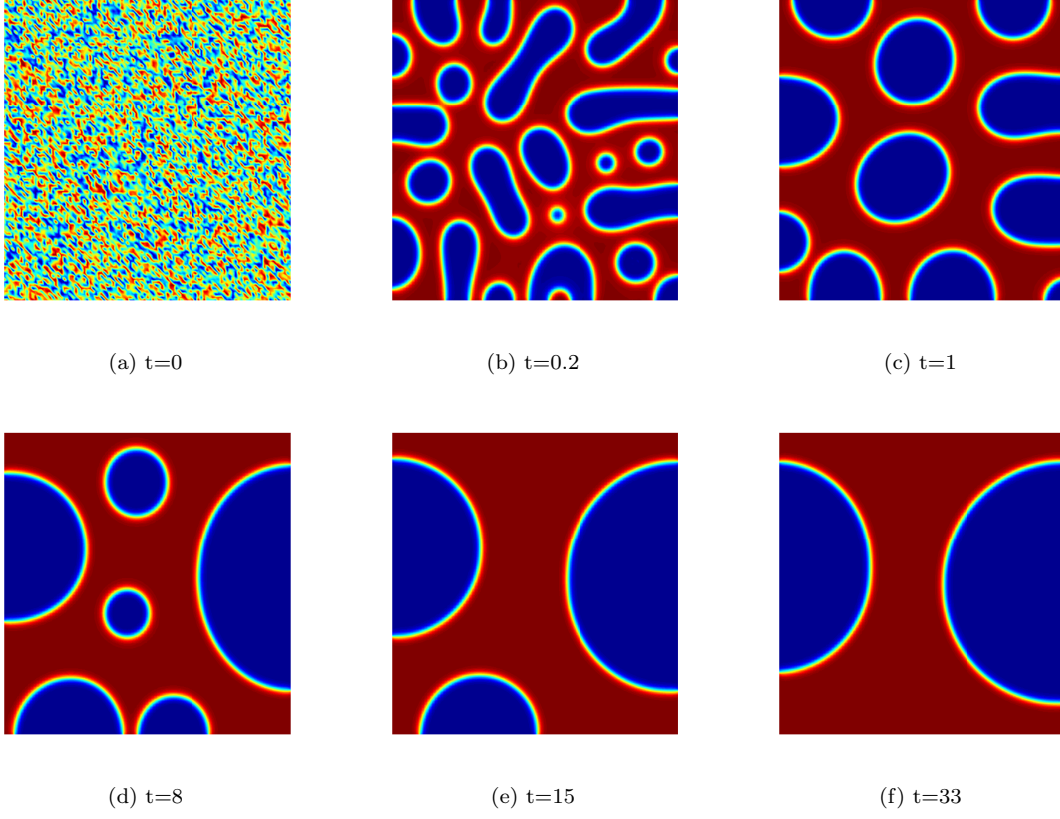


Figure 5: Snapshots of the phase variable ϕ at $t = 0, 0.2, 1, 8, 15, 33$ with $\phi_a = 0.1, \phi_b = 0.001$ for **Example 3**

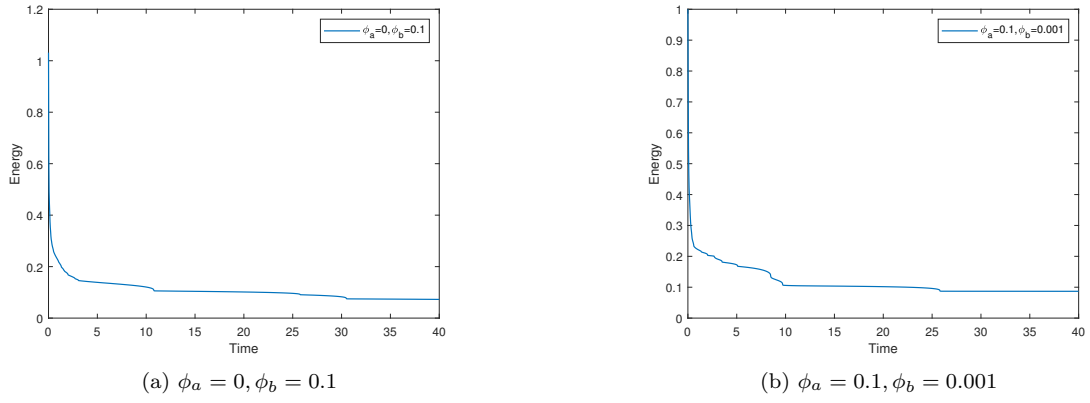


Figure 6: Time evolution of the original discrete free energy functional (26) for the coarsening dynamic model with (a) $\phi_a = 0, \phi_b = 0.1$; (b) $\phi_a = 0.1, \phi_b = 0.001$.

References

- [1] Georgios Akrivis, Buyang Li, and Dongfang li. Energy-decaying extrapolated rk-sav methods for the allen-cahn and cahn-hilliard equations. *SIAM Journal on Scientific Computing*, 41:A3703–A3727, 2019.
- [2] Andrew J. Archer and Markus Rauscher. Dynamical density functional theory for interacting Brownian particles: stochastic or deterministic? *Journal of Physics A General Physics*, 37:9325–9333, 2004.
- [3] Nicola J. Armstrong, Kevin J. Painter, and Jonathan A. Sherratt. A continuum approach to modelling cell-cell adhesion. *Journal of theoretical biology*, 243:98–113, 2006.
- [4] Nicola J. Armstrong, Kevin J. Painter, and Jonathan A. Sherratt. Adding Adhesion to a Chemical Signaling Model for Somite Formation. *Bulletin of Mathematical Biology*, 71:1–24, 2009.
- [5] Peter W. Bates. On some nonlocal evolution equations arising in materials science. Nonlinear dynamics and evolution equations. *Fields Institute Communications*, 48:13–52, 2006.
- [6] Peter W. Bates and Jianlong Han. The Dirichlet boundary problem for a nonlocal Cahn-Hilliard equation. *Journal of Mathematical Analysis and Applications*, 311:289–312, 2005.
- [7] Peter W. Bates and Jianlong Han. The Neumann boundary problem for a nonlocal Cahn-Hilliard equation. *Journal of Differential Equations*, 212:235–277, 2005.
- [8] John W. Cahn and John E. Hilliard. Free Energy of a Nonuniform System. I. Interfacial Free Energy. *Journal of Chemical Physics*, 28:258–267, 1958.
- [9] Arnaud Chauviere, Haralambos Hatzikirou, Ioannis G. Kevrekidis, John S. Lowengrub, and Vittorio Cristini. Dynamic density functional theory of solid tumor growth: Preliminary models. *AIP advances*, 2:8032–234, 2012.
- [10] Chuanjun Chen and Xiaofeng Yang. Highly efficient and unconditionally energy stable semi-discrete time-marching numerical scheme for the two-phase incompressible flow phase-field system with variable-density and viscosity. *Science China Mathematics*, 65:1–26, 2022.
- [11] Longqing Chen and Yunzhi Wang. The continuum field approach to modeling microstructural evolution. *JOM*, 48:13–18, 1996.
- [12] Pierluigi Colli, Sergio Frigeri, and Maurizio Grasselli. Global existence of weak solutions to a nonlocal Cahn-Hilliard-Navier-Stokes system. *Journal of Mathematical Analysis and Applications*, 386:428–444, 2011.
- [13] Qiang Du, Max D. Gunzburger, Richard B. Lehoucq, and Kun Zhou. Analysis and Approximation of Nonlocal Diffusion Problems with Volume Constraints. *SIAM Review*, 54:667–696, 2012.
- [14] Qiang Du, Lili Ju, Xiao Li, and Zhonghua Qiao. Stabilized linear semi-implicit schemes for the nonlocal cahn-hilliard equation. *Journal of Computational Physics*, 363:39–54, 2018.
- [15] Robert Evans. The nature of the liquid-vapour interface and other topics in the statistical mechanics of non-uniform, classical fluids. *Advances in Physics*, 28:143–200, 1979.

- [16] Herbert Gajewski and Klaus Gärtner. On a nonlocal model of image segmentation. *Zeitschrift für angewandte Mathematik und Physik ZAMP*, 56:572–591, 2005.
- [17] Giambattista Giacomini and Joel L Lebowitz. Phase segregation dynamics in particle systems with long range interactions. I. Macroscopic limits. *Journal of Statistical Physics*, 87:37–61, 1997.
- [18] Giambattista Giacomini and Joel L Lebowitz. Phase Segregation Dynamics in Particle Systems with Long Range Interactions II: Interface Motion. *SIAM Journal on Applied Mathematics*, 58:1707–1729, 1998.
- [19] Yuezheng Gong, Jia Zhao, and Qi Wang. Arbitrarily high-order unconditionally energy stable sav schemes for gradient flow models. *Computer Physics Communications*, 249:107033, 2020.
- [20] Zhen Guan, John S. Lowengrub, Cheng Wang, and Steven M. Wise. Second order convex splitting schemes for periodic nonlocal Cahn-Hilliard and Allen-Cahn equations. *Journal of Computational Physics*, 277:48–71, 2014.
- [21] Zhen Guan, Cheng Wang, and Steven M. Wise. A convergent convex splitting scheme for the periodic nonlocal Cahn-Hilliard equation. *Numerische Mathematik*, 128:377–406, 2014.
- [22] Dianming Hou, Mejdi Azaiez, and Chuanju Xu. A variant of scalar auxiliary variable approaches for gradient flows. *Journal of Computational Physics*, 395:307–332, 2019.
- [23] Fukeng Huang and Jie Shen. A new class of implicit-explicit bdf k sav schemes for general dissipative systems and their error analysis. *Computer Methods in Applied Mechanics and Engineering*, 392:114718, 2022.
- [24] Maryna Kapustina, Denis Tsygankov, Jia Zhao, Timothy Wessler, Xiaofeng Yang, Alex Chen, Nathan P Roach, Timothy C. Elston, Qi Wang, Ken Jacobson, and M. Gregory Forest. Modeling the Excess Cell Surface Stored in a Complex Morphology of Bleb-Like Protrusions. *PLoS Computational Biology*, 12:e1004841, 2016.
- [25] Christos N. Likos, Bianca M. Mladek, Dieter Gottwald, and Gerhard Kahl. Why do ultrasoft repulsive particles cluster and crystallize? Analytical results from density-functional theory. *The Journal of chemical physics*, 126:224502, 2007.
- [26] Chun Liu and Jie Shen. A phase field model for the mixture of two incompressible fluids and its approximation by a Fourier-spectral method. *Physica D: Nonlinear Phenomena*, 179:211–228, 2003.
- [27] Huan Liu, Aijie Cheng, Hong Wang, and Jia Zhao. Time-fractional Allen-Cahn and Cahn-Hilliard phase-field models and their numerical investigation. *Computers & Mathematics with Applications*, 76:1876–1892, 2018.
- [28] Zhengguang Liu and Xiaoli Li. The Exponential Scalar Auxiliary Variable (E-SAV) Approach for Phase Field Models and Its Explicit Computing. *SIAM Journal on Scientific Computing*, 42:B630–B655, 2020.
- [29] Zhengguang Liu and Xiaoli Li. The fast scalar auxiliary variable approach with unconditional energy stability for nonlocal Cahn-Hilliard equation. *Numerical Methods for Partial Differential Equations*, 37:244–261, 2020.

- [30] Zhengguang Liu and Xiaoli Li. A highly efficient and accurate exponential semi-implicit scalar auxiliary variable (ESI-SAV) approach for dissipative system. *Journal of Computational Physics*, 447:110703, 2021.
- [31] John S. Lowengrub, Andreas Rätz, and Axel Voigt. Phase-field modeling of the dynamics of multicomponent vesicles: Spinodal decomposition, coarsening, budding, and fission. *Physical review. E, Statistical, nonlinear, and soft matter physics*, 79:031926, 2009.
- [32] Umberto Marini Bettolo Marconi and Pedro Tarazona. Dynamic density functional theory of fluids. *The Journal of Chemical Physics*, 110:8032–8044, 1999.
- [33] R. C. Merton. Option pricing when underlying stock returns are discontinuous. *Journal of Financial Economics*, 3:125–144, 1976.
- [34] C. Miehe, Martina Hofacker, and Fabian Welschinger. A phase field model for rate-independent crack propagation: Robust algorithmic implementation based on operator splits. *Computer Methods in Applied Mechanics and Engineering*, 199:2765–2778, 2010.
- [35] Len M Pismen. Nonlocal diffuse interface theory of thin films and the moving contact line. *Physical Review E*, 64:021603, 2001.
- [36] Robert C. Rogers. A nonlocal model for the exchange energy in ferromagnetic materials. *Journal of Integral Equations and Applications*, 3:85–127, 1991.
- [37] Robert C. Rogers. Some remarks on nonlocal interactions and hysteresis in phase transitions. *Continuum Mechanics and Thermodynamics*, 8:65–73, 1994.
- [38] Jie Shen, Jie Xu, and Jiang Yang. The scalar auxiliary variable (SAV) approach for gradient flows. *Journal of Computational Physics*, 353:407–416, 2018.
- [39] Jie Shen and Xiaofeng Yang. Numerical approximations of Allen-Cahn and Cahn-Hilliard equations. *Discrete and Continuous Dynamical Systems*, 28:1669–1691, 2010.
- [40] Zengqiang Tan and Huazhong Tang. A general class of linear unconditionally energy stable schemes for the gradient flows. *Journal of Computational Physics*, 464:111372, 2022.
- [41] Zhifeng Weng, Shuying Zhai, and Xinlong Feng. Analysis of the operator splitting scheme for the Cahn-Hilliard equation with a viscosity term. *Numerical Methods for Partial Differential Equations*, 35:1949–1970, 2019.
- [42] Xufeng Xiao, Xinlong Feng, and Jinyun Yuan. The stabilized semi-implicit finite element method for the surface Allen-Cahn equation. *Discrete and Continuous Dynamical Systems-series B*, 22:2857–2877, 2017.
- [43] Xiaofeng Yang and Jia Zhao. Efficient linear schemes for the nonlocal Cahn-Hilliard equation of phase field models. *Computer Physics Communications*, 235:234–245, 2018.